

Pressure-Induced Coordination–Structural Change around Zinc(II) in Zinc(II)-Neutralized Ethylene–Methacrylic Acid Ionomers. 1. Infrared Spectroscopic Studies

Shoichi Kutsumizu,^{*,†} Muneatsu Nakamura,[‡] and Shinichi Yano^{*,‡}

Instrumental Analysis Center, Gifu University, Yanagido 1-1, Gifu 501-1193, Japan, and Department of Chemistry, Faculty of Engineering, Gifu University, Yanagido 1-1, Gifu 501-1193, Japan

Received August 1, 2000; Revised Manuscript Received January 3, 2001

ABSTRACT: The coordination structure around zinc(II) in a 60% neutralized zinc(II) salt of ethylene–methacrylic acid (E-MAA) ionomer was investigated by infrared (IR) spectroscopic studies. It was found that the IR carboxylate antisymmetric stretching ($\nu_{\text{as}}(\text{COO}^-)$) band profile, and thus the coordination structure around zinc(II), strongly depends on the pressure (P) applied at 403 K in the melt: When the sample was placed at 403 K under vacuum (i.e., $P = 0$), two $\nu_{\text{as}}(\text{COO}^-)$ bands at 1624 and 1538 cm^{-1} were observed and ascribed to hexacoordination structures of zinc(II) carboxylates, but increasing P intensified a sharp $\nu_{\text{as}}(\text{COO}^-)$ band at 1585 cm^{-1} , assigned to a tetracoordination structure. A remarkable feature of this pressure-induced coordinational change is that even exposure to atmospheric pressure ($P = 0.1$ MPa) is enough to change the coordination structure significantly. The coordinational change was found to be dependent on the temperature at which the pressure was applied below the melting temperature (~ 357 K) of the polyethylene crystalline region, which is considered to act as a physical cross-link, thus constraining the transformation of the coordination structure.

Introduction

Ionomers contain a small number of ionic groups which are chemically incorporated into a hydrophobic matrix, and the ionic groups tend to form ion-rich domains of nanometer size (hereafter simply called ionic aggregates) in the matrix.¹ It is the formation of ionic aggregates that markedly improves the material properties such as mechanical strength and elasticity, clarity, moldability, etc., compared with the host polymer. Actually, poly(ethylene-*co*-methacrylic acid) [E-MAA]-based ionomers are commercially very important for use in molding and packaging applications. Therefore, from both fundamental and industrial points of view, extensive work has been devoted to understanding the local environment inside the ionic aggregates as well as the size, shape, and distribution in space of the aggregates. Information on the size, shape, and distribution in space of ionic aggregates is primarily given by small-angle X-ray scattering (SAXS),² and in E-MAA ionomers, the number of ionic groups incorporated into an ionic aggregate was estimated at 6–12 for the sodium salts whereas at only 3–4 for the zinc salts.³ The local environment inside the aggregates is usually investigated by infrared (IR),⁴ electron spin resonance (ESR),⁵ extended X-ray absorption fine structure (EXAFS)⁶ spectroscopies, and others. One important conclusion from these studies is that the coordination structure around the neutralizing cations in ionomers in most cases is similar to that of the corresponding low-molecular-mass metal carboxylates. However, examples have also been reported that the coordination structure and properties of some transition-metal carboxylates in E-MAA ionomers are different from those of the low-molecular-mass analogues. For example, manganese-

(II)–organic amine complexes^{7,8} and cobalt(II) salts^{9,10} of E-MAA show selective oxygen gas absorption, which is a function produced by introducing the metal carboxylates into the ionomeric matrix.

In zinc(II)-neutralized E-MAA ionomers, information on the local environment around zinc(II) is available from IR^{11–14} and EXAFS^{6,15–19} studies, and it has been revealed that the coordination structure around zinc(II) is sensitively changed with temperature^{11,13,15} and water absorption,^{12,18} but there still remain several controversies. Very recently, we found an interesting phenomenon that the coordination structure around zinc(II) is primarily determined by pressure applied at 403 K in the melt.^{13,19} When the pressure is zero (i.e., the sample is placed in vacuo) in the melt, the zinc(II) carboxylates preferentially form a hexacoordination structure, which is characterized by two IR carboxylate antisymmetric stretching ($\nu_{\text{as}}(\text{COO}^-)$) bands at 1624 and 1538 cm^{-1} , but increasing the pressure favors a tetracoordination structure with a sharp $\nu_{\text{as}}(\text{COO}^-)$ band at 1585 cm^{-1} (see also Figure 1). A remarkable feature is that even exposure to atmospheric pressure ($P = 0.1$ MPa) is enough to change the coordination structure largely, which will be described in this paper. As will be reported in the forthcoming paper, such pressure effects on the coordination structure around zinc(II) are characteristic of zinc(II) carboxylates surrounded by a polymer backbone and quite dependent upon the ionomeric composition and the degree of neutralization; in E-MAA ionomers, the pressure effect is most marked for the 60% neutralized salt of E-MAA with a MAA content of 5.4 mol %, denoted as E-0.054MAA-0.6Zn hereafter. Since such pressure-induced coordinational change is not seen for the low-molecular-mass zinc(II) carboxylates, it is unique and intriguing as a property that is functionalized in the ionomeric matrix.

The aim of this paper is to investigate the pressure effect on the coordination structure of zinc(II) carboxylates in E-0.054MAA-0.6Zn by using IR spectroscopic

[†] Instrumental Analysis Center.

[‡] Department of Chemistry, Faculty of Engineering.

* To whom correspondence should be addressed. E-mail: kutsu@cc.gifu-u.ac.jp; yano@apchem.gifu-u.ac.jp.

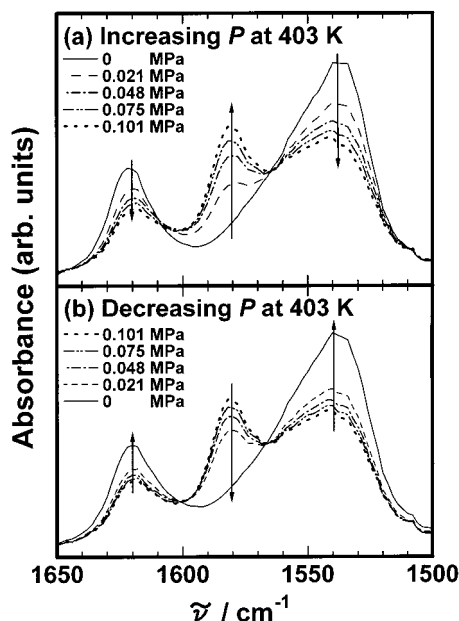


Figure 1. Infrared (IR) spectra of E-0.054MAA-0.6Zn in the carboxylate antisymmetric stretching [$\nu_{as}(\text{COO}^-)$] band region measured at 403 K as a function of applied pressure P . (a) and (b) are the variations when P is increased and decreased, respectively, where arrows represent the directions of the variations of three IR peaks. The pressure medium was dry N_2 (0.101 MPa = 760 mmHg = 1 atm).

techniques. The results are discussed in terms of a simple equilibrium shift upon pressure between tetra- and hexacoordination states of zinc(II). The effect of the temperature at which the pressure is applied below the melting temperature is also mentioned. Selected preliminary results have been presented.¹³

Experimental Section

E-0.054MAA-0.6Zn, which was prepared by a melt reaction of E-MAA with zinc oxide as described previously,²⁰ was kindly given to us in pelletized form by Technical Center, Du Pont-Mitsui Polychemicals Co., Ltd., Chiba, Japan. The degree of neutralization was confirmed by a decrease in intensity of IR carbonyl stretching ($\nu(\text{C}=\text{O})$) band at 1698 cm^{-1} . The pellet samples were first compression-molded at 403 K and at 200 kg/cm^2 (instrumental value), transformed into ~ 30 μm thick films, and then vacuum-dried at 403 K for 2 h using a rotary pump (pressure $P = 7 \times 10^{-4}$ MPa) and cooled to room temperature in 2 h (cooling rate ~ 1 K min^{-1}). The films obtained in this way were used as the starting sample for IR measurements. The IR spectra were recorded with a Perkin-Elmer 1640 FT-IR spectrometer in the following two measuring procedures, where each trace was taken as the average of 16 scans at a resolution of 4 cm^{-1} .

(E-1) IR Spectra under a Relatively Low Pressure below 0.101 MPa. A commercial gas cell (GL Sciences Co., Tokyo, Type GC-KBr) equipped with a handmade heater and a calibrated iron-constantan thermocouple was used, and the starting film was placed between two KBr windows of the gas cell. The temperature was maintained by regulating the heater current from a Takasago GP035-15R dc power supply with an Okura EC5918A13 controller, and the pressure was controlled with dry N_2 gas. The IR spectra were recorded at various temperatures and pressures (but below 0.101 MPa).

(E-2) IR Spectra under High Pressure above 0.101 MPa. The starting film was put into an autoclave, which was filled by dry N_2 gas to adjust the pressure. The autoclave was heated to 403 K and annealed for 2 h and then cooled to room temperature at a rate of about 3 K min^{-1} . After that, the IR spectra were recorded at 303 K.

In most experiments, the temperature at which the pressure is applied was 403 K, and above the temperature, a trace of peaks at 1802, 1780, 1750, and 1735 cm^{-1} was detected and related to the formation of anhydrous carboxylates.²¹ The physical meaning of the temperature 403 K is discussed later in the Results and Discussion section.

Digital encoding of the spectral data was carried out at 2 cm^{-1} intervals and transferred into an EPSON PC-486GR personal computer with an i486SX microprocessor for further calculations described below: The baseline of each spectrum was assumed to be a line through two minimum points: one in the region 450–1700 cm^{-1} and the other in 1700–2000 cm^{-1} . After the baseline subtraction, the spectrum in the region 1500–1650 cm^{-1} was resolved into four peaks by using a modified version of the curve-fitting program originally written by Minami²² as a BASIC program. The program includes a Davidson–Fletcher–Powell optimization routine,²³ and each absorption peak was given by a Gauss–Lorentz function^{24,25} as

$$F(\nu) = H \exp[-\ln 2((\nu_0 - \nu)/W_1)^2] / (1 + ((\nu_0 - \nu)/W_2)^2) \quad (1)$$

where ν_0 (peak frequency), H (peak intensity at ν_0), W_1 (half-bandwidth at half-maximum in Gaussian component), and W_2 (half-bandwidth at half-maximum in Lorentzian component) are adjustable parameters.

Results and Discussion

Coordination Change of Zinc(II) Carboxylates with Pressure Applied in the Melt. Figure 1 shows IR spectra of E-0.054MAA-0.6Zn at 403 K as a function of applied pressure P , where dry N_2 gas was used as a pressure medium and the measuring procedure E-1 was employed. As the pressure is increased from $P = 0$ to 0.1 MPa, in (a), two $\nu_{as}(\text{COO}^-)$ bands at 1624 and 1538 cm^{-1} are diminished and a peak at 1585 cm^{-1} newly appears and is intensified. When the pressure is decreased from 0.1 MPa, in (b), then, the reverse trend is observed, with a small hysteresis. Two isosbestic points at around 1605 and 1565 cm^{-1} are clearly visible, suggesting that this pressure-induced transformation occurs between (at least) two distinct coordination states of zinc(II) carboxylates, where one is related to the two bands at 1624 and 1538 cm^{-1} and the other to the 1585 cm^{-1} band, and increasing the pressure favors the latter coordination state. Ishioka et al.¹² and Grady et al.¹⁸ pointed out the possibility of water absorption affecting the coordination structure around zinc(II) in E-MAA ionomers. However, the transformation of the coordination structure shown in Figure 1 is not due to the water absorption because the transformation takes place at 403 K above the boiling point of water.

Figure 2 shows the variations of spectral patterns during cooling from the melt (at ~ 410 K) under constant pressures of (a) $P = 0$ and (b) $P = 0.1$ MPa (= 1 atm = 760 mmHg). Under both pressures, as the temperature is decreased to 310 K, a peak at 1750 cm^{-1} is diminished while two peaks at 1700 and 1466 cm^{-1} are sharpened and intensified. The 1750 and 1700 cm^{-1} bands are assigned to the carbonyl stretching [$\nu(\text{C}=\text{O})$] bands for monomeric and dimeric COOH groups, respectively, and thus, the observed change is associated with the formation of hydrogen-bonded COOH dimers from the monomers. The 1466 cm^{-1} is assigned to CH_2 bending [$\delta(\text{CH}_2)$] band from both crystalline and amorphous polyethylene regions, and the intensification during the cooling is due to the crystallization of polyethylene segments from the melt. In the $\nu_{as}(\text{COO}^-)$ band region of 1650–1500 cm^{-1} , the spectral change during the

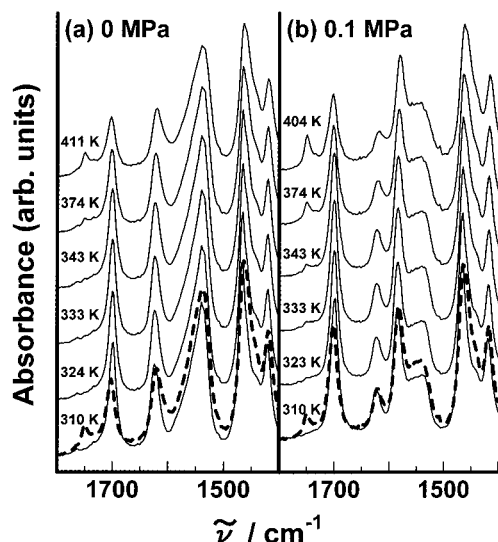


Figure 2. Variations of IR spectra in the region 1800–1400 cm^{-1} during cooling from 411/404 K under a constant pressure of (a) 0 (i.e., under vacuum) and (b) 0.1 MPa of dry N_2 (i.e., the atmospheric pressure of 760 mmHg). At the same place of the spectrum at 310 K, the spectrum at 411/404 K is also drawn as a bold broken curve for easy comparison.

cooling is very small; the band profile at 310 K (which is drawn as a thin solid curve) is slightly sharper than the corresponding profile at ~ 410 K (drawn as a bold broken curve at the same position of the 310 K profile). Neglecting such small changes, it can be said that the $\nu_{\text{as}}(\text{COO}^-)$ band profile at 310 K almost copies the profile in the melt when the pressure is kept constant during the cooling to 310 K. In other words, the spectral changes with varying the pressure in the melt are directly reflected to the room-temperature patterns, which allows us the measuring procedure E-2. This is further confirmed by comparing the results of two measuring procedures E-1 and E-2 in Figure 3, where the peak intensity of each band is normalized with respect to the $\delta(\text{CH}_2)$ band at 1466 cm^{-1} . One can see that the pressure dependences of the peak intensities of three bands at 1624, 1585, and 1538 cm^{-1} are essentially the same between the two procedures; the intensities of the 1624 and 1538 cm^{-1} bands decrease, while that of the 1585 cm^{-1} band increases, with increasing the pressure P .

Figure 4 examines the pressure effect on the coordination structure around zinc(II) by using two pressure mediums, nitrogen and argon, in the E-2 procedure. Clearly, the two pressure mediums gave no difference in the pressure effect on the spectral pattern and hence on the coordination structure around zinc(II). This result confirms that two gases certainly act as a pressure medium.

Figure 5 presents the variation of the $\nu_{\text{as}}(\text{COO}^-)$ band profile with applied pressure in the melt, where the pressure ranges from vacuum ($P = 0$) to $P = 5$ MPa and the spectra were obtained from the E-2 procedure. Intensification of the 1585 cm^{-1} band with increasing P continues above $P = 0.1$ MPa, but the spectra at $P = 4$ and 5 MPa (spectra 8 and 9 in Figure 5, respectively) are completely overlapped with each other, which implies that the pressure effect on the coordination structure around zinc(II) is virtually saturated in that pressure range. It is also concluded that even exposure to atmospheric pressure ($P = 0.1$ MPa) is enough to

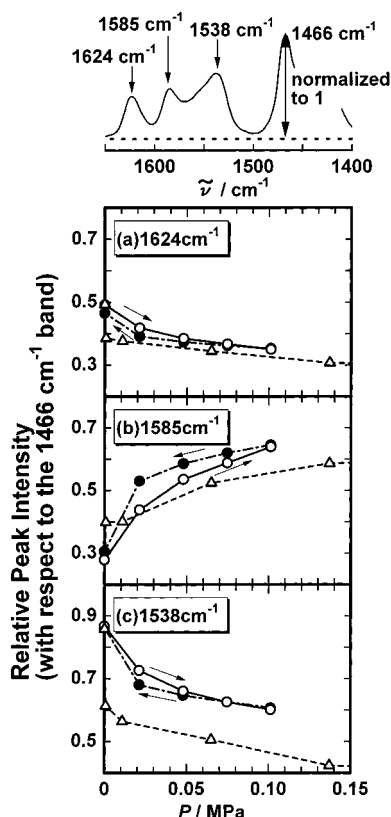


Figure 3. Comparisons of two measuring procedures E-1 (\circ — \circ —, \bullet — \bullet —) and E-2 (\triangle — \triangle —): variations of relative peak intensities of (a) 1624, (b) 1585, and (c) 1538 cm^{-1} bands with pressure (P) applied at 403 K. Each intensity is normalized with respect to that of the 1466 cm^{-1} band, as illustrated at the top.

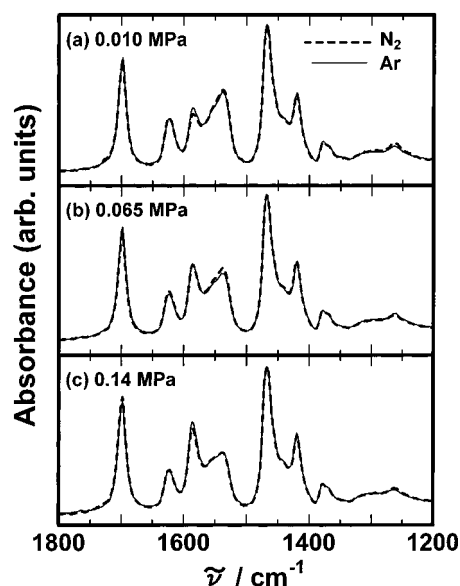


Figure 4. Comparisons of two pressure mediums N_2 (broken curve) and Ar (solid curve) in the region 1800–1200 cm^{-1} : the values of the pressure applied at 403 K are (a) 0.010, (b) 0.065, and (c) 0.14 MPa.

change the coordination structure largely, as seen in spectrum 5. Furthermore, the film obtained by compression-molding at 403 K and at 200 kg/cm^2 ($=19.6$ MPa, but is an instrumental value) showed the same pattern with spectrum 8 or 9, which excludes again the possibility of gas permeation in the melt changing the coordination structure around zinc(II).

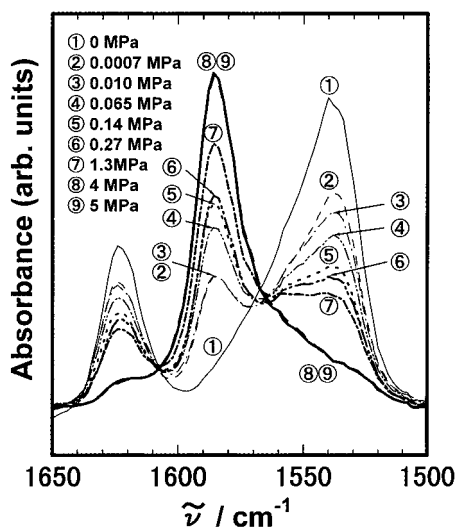


Figure 5. Variation of IR spectra in the $\nu_{\text{as}}(\text{COO}^-)$ band region with pressure applied at 403 K. The measuring procedure E-2 was employed; that is, the pressure denoted in MPa was applied at 403 K for 2 h, cooled to room temperature keeping the pressure, and after that, the spectra were recorded at room temperature.

According to Coleman et al.,¹¹ the band at 1585 cm^{-1} is assigned to a tetracoordination structure around zinc(II), and this assignment is also supported by EXAFS studies.^{6,15,16,18} The assignment of the 1538 and 1624 cm^{-1} bands, on the other hand, is still a subject of debate. Coleman et al.¹¹ assigned these two bands to an acid salt structure whose coordination number around zinc(II) is apparently larger than 4 and the 1565 cm^{-1} band, which is not so evident in Figure 1 or 5 but certainly exists, to a hexacoordination structure around zinc(II). Ishioka¹² and Grady and co-workers¹⁸ assigned these three bands to a tetracoordination structure of zinc(II) with some of the oxygen atoms of the carboxylate groups replaced by those of water molecules because of water absorption of the sample. Although our work never denies the possibility of water absorption affecting the coordination structure around zinc(II) under their experimental conditions, it has demonstrated that the transformation of the coordination structure around zinc(II) does not necessarily need water absorption. Therefore, it is concluded at this stage that the assignment by Coleman et al. is more plausible, and it is more realistic to consider that various types of coordination structures are present in the sample from tetra- to hexacoordination structures, including Coleman's type; the hexacoordination structure in the form $(-\text{COO}^-)_2\text{-Zn(II)}$ is regarded as an ultimate structure. In this meaning, we simply assign three bands at 1538 , 1565 , and 1624 cm^{-1} all to hexacoordination structures around zinc(II). Our preliminary EXAFS studies showed that the coordination number in the first coordination shell around zinc(II) certainly decreases from 4.8 to 3.0 with increasing the pressure in the melt from $P = 0$ to 4 MPa.¹⁹ This and the IR results support our interpretation that the pressure in the melt affects an equilibrium between the hexacoordinated and tetracoordinated zinc(II) in this ionomer, and increasing the pressure makes the presence of the latter species more abundant.

Temperature at Which Pressure Applied. The pressure behavior at 323 K is presented in Figure 6, where the film of E-0.054MAA-0.6Zn was first vacuum-dried at 403 K for 2 h, and then the pressure was applied at 323 K. After 2 h, the sample was cooled to

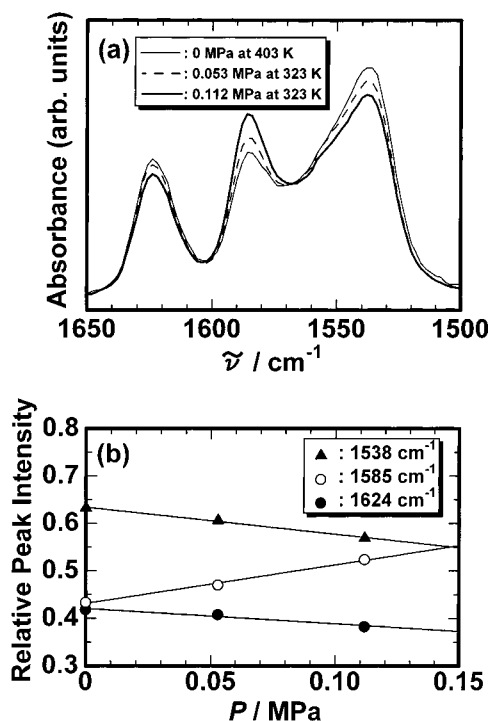


Figure 6. (a) Variation of IR spectra in the $\nu_{\text{as}}(\text{COO}^-)$ band region with pressure applied at 323 K. The spectrum denoted as "0 MPa at 403 K" is the starting sample before the application of pressure at 323 K. (b) Variations of relative peak intensities of 1538 (▲), 1585 (○), and 1624 cm^{-1} (●) bands with pressure (P) applied at 323 K. Each intensity is normalized with respect to that of the 1466 cm^{-1} band, as in Figure 3.

room temperature, keeping the pressure, and the IR spectrum was recorded as in the E-2 procedure. As shown in (a), the spectra exhibited a pressure change similar to that observed at 403 K; the 1585 cm^{-1} band is intensified while the 1624 and 1538 cm^{-1} bands are diminished with increasing the pressure P at 323 K. In (b), the spectra are normalized with respect to the absorbance of the $\delta(\text{CH}_2)$ band at 1466 cm^{-1} , and the absorbances (A) of three $\nu_{\text{as}}(\text{COO}^-)$ bands at 1538 , 1585 , and 1624 cm^{-1} are plotted as a function of P at 323 K. In a limited pressure range such as from $P = 0$ to 0.15 MPa, the changes are approximated to be linear with P , as in the case of Figure 3. The slope ($\Delta A/\Delta P$) of this plot represents the magnitude of change with pressure. For all three $\nu_{\text{as}}(\text{COO}^-)$ bands, the absolute value $|\Delta A/\Delta P|$ at 323 K is smaller than the corresponding value at 403 K.

In the present work, the starting sample of E-0.054MAA-0.6Zn was vacuum-dried at 403 K for 2 h before applying the pressure, as described in the Experimental Section. The DSC heating curve of the sample is displayed in Figure 7a, which shows a broad endothermic peak centered at 357 K, assigned to the melting of polyethylene crystalline region and denoted as T_m . Since the sample was measured immediately after cooling from 403 K as in the E-2 procedure, another endothermic peak assigned to an order-disorder transition of ionic aggregate regions in this ionomer,^{14,26} which is observed at around 325 K for the same sample stored at room temperature for a few days, is not visible in the figure. Figure 7b shows how the values of $\Delta A/\Delta P$ for three $\nu_{\text{as}}(\text{COO}^-)$ bands at 1538 , 1585 , and 1624 cm^{-1} depend on the temperature at which pressure is applied. The $\Delta A/\Delta P$ of the 1585 cm^{-1} band increases while those of the 1624 and 1538 cm^{-1} bands decrease with increas-

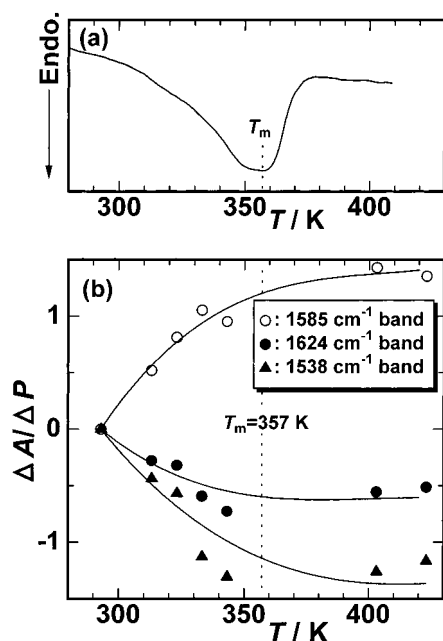


Figure 7. (a) DSC heating curve of the starting sample before the application of pressure. T_m denotes the melting temperature (357 K) of polyethylene crystalline region in the sample. (b) Plots of $\Delta A/\Delta P$ of three $\nu_{as}(\text{COO}^-)$ bands at 1585 (\circ), 1624 (\bullet), and 1538 cm^{-1} (\blacktriangle) vs application temperature of pressure P . $\Delta A/\Delta P$ is the slope of the absorbance (A) vs P plots between $P = 0$ and 0.15 MPa, where each A is normalized with the 1466 cm^{-1} band, and the solid curves are only guides for the eye.

ing the application temperature of pressure, but all three are leveled off at around T_m . This result clearly indicates that the polyethylene crystalline region acts as a physical cross-link of the backbone and severely constrains the transformation of the coordination structure around zinc(II) with varying pressure at low temperatures near room temperature. This is also the reason the $\nu_{as}(\text{COO}^-)$ band profile of the zinc(II)-neutralized E-MMA ionomer, and thus the coordination structure around zinc(II), remains unchanged when the pressure is released and/or reverted to the atmospheric pressure at room temperature in the E-2 procedure. Above T_m , such constraint is removed, and the structure around zinc(II) responds freely and sensitively to the applied pressure. Of course, the change is considered to be an equilibrium process with temperature above T_m as well as pressure, and the detailed studies on the activation energy are currently progressing, although temperature would have apparently a smaller effect on the coordination structure around zinc(II).

Resolution of IR $\nu_{as}(\text{COO}^-)$ Band Profile and Comparison with EXAFS Results. To obtain a more quantitative information on the pressure behavior of each $\nu_{as}(\text{COO}^-)$ band, the spectral pattern in the region 1650–1500 cm^{-1} was resolved into four band components. The result is presented in Figure 8. In the curve-fitting procedure, a band at around 1560 cm^{-1} was added in addition to the three bands at 1624, 1585, and 1538 cm^{-1} discussed above. The existence of the 1560 cm^{-1} band is clearly suggested from the spectral shapes for mid four pressure values from (c) to (f). Although the adjustment of the 1560 cm^{-1} band parameters may contain some error for two extreme cases of (a) and (g), the fittings are fairly good for all cases. The obtained adjustable parameters are listed in Table 1. For all four bands, the peak frequency value ν_0 determined by the

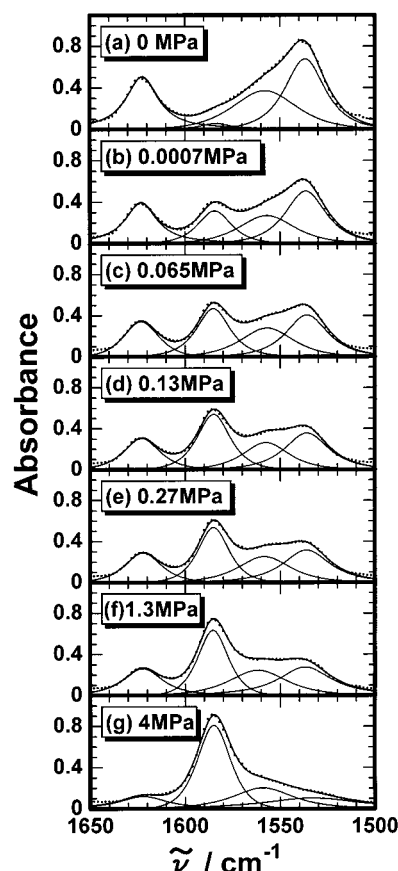


Figure 8. Curve-fitting results for the spectra obtained by the E-2 procedure, where dotted curves are observed spectra, and thin solid and solid curves are component spectra and the sum of the four component spectra, respectively. The details of the E-2 procedure and the curve-fitting procedure are described in the Experimental Section.

fittings is somewhat different from that obtained from the observed spectral profile; ν_0 of the 1624, 1585, 1560, and 1538 cm^{-1} bands is 1622 ± 1 , 1585 ± 1 , 1558 ± 1 , and 1536 ± 1 cm^{-1} , respectively. Hereafter in this paper, these four bands are referred to by using these ν_0 values.

On the basis of the fitting results, the integrated absorbances of the four $\nu_{as}(\text{COO}^-)$ band components were calculated, where the total integrated absorbance was normalized to 1. Assuming that the molar absorption coefficients for the four components are all identical and all the components themselves represent a coordination state around zinc(II), the normalized integrated absorbance of each component corresponds to the fraction of the state. Figure 9 shows the plots of the fractions estimated in this way as a function of pressure P applied at 403 K in the melt. As the pressure is increased, the fraction of the 1585 cm^{-1} band component increases, while both 1622 and 1536 cm^{-1} band components decrease. Such changes are initially rapid up to around $P = 0.25$ MPa, beyond which they become gentle. On the other hand, the 1558 cm^{-1} band component did not show a marked pressure dependence in the whole range.

The fact that the integrated absorbances of both 1622 and 1536 cm^{-1} band components show a similar pressure dependence whereas the pressure behavior of the 1558 cm^{-1} band component is quite different from those of the former two is consistent with the assignment by Coleman et al. that the former two and the 1558 cm^{-1} band components correspond to different coordination states: the former two to an acid salt structure of

Table 1. E-0.054MAA-0.6Zn: Band Position (ν_0/cm^{-1}), Peak Height (H), and Half-Bandwidths at Half-Maximum in Gaussian Component (W_1/cm^{-1}) and in Lorentzian Component (W_2/cm^{-1}) at Various Pressures at 403 K^a

press./ MPa	1622 cm^{-1} band				1585 cm^{-1} band				1558 cm^{-1} band				1536 cm^{-1} band			
	ν_0/cm^{-1}	H	W_1/cm^{-1}	W_2/cm^{-1}	ν_0/cm^{-1}	H	W_1/cm^{-1}	W_2/cm^{-1}	ν_0/cm^{-1}	H	W_1/cm^{-1}	W_2/cm^{-1}	ν_0/cm^{-1}	H	W_1/cm^{-1}	W_2/cm^{-1}
0	1622.4	0.502	217.4	10.2	1583.8	0.056	25.2	10.1	1558.1	0.370	33.5	25.6	1536.9	0.676	28.2	14.1
0.0007	1623.1	0.392	136.6	10.1	1584.4	0.315	21.5	12.0	1557.0	0.268	30.6	21.2	1536.6	0.505	29.5	14.2
0.010	1623.1	0.384	111.7	10.1	1584.7	0.316	22.7	13.1	1557.4	0.261	28.6	18.9	1536.7	0.477	33.1	14.6
0.065	1623.0	0.341	18.9	13.7	1585.1	0.467	24.1	11.7	1556.9	0.278	30.3	19.8	1536.0	0.405	31.1	14.4
0.14	1622.8	0.305	24.2	12.8	1585.0	0.539	21.3	12.0	1557.5	0.263	29.2	16.6	1536.1	0.356	34.1	15.1
0.27	1622.1	0.288	23.8	13.1	1585.1	0.535	18.8	11.5	1558.4	0.252	33.2	19.0	1536.3	0.315	41.4	15.8
1.3	1622.3	0.262	34.0	13.1	1585.4	0.637	17.1	11.7	1561.8	0.245	36.2	21.0	1537.1	0.278	63.7	17.1
4	1622.1	0.120	58.8	15.6	1585.0	0.809	18.1	13.0	1559.3	0.202	42.7	21.3	1533.2	0.103	113.6	31.0
5	1621.7	0.109	64.0	16.4	1585.1	0.789	17.2	12.0	1559.3	0.198	43.6	26.4	1536.1	0.084	125.3	50.5

^a All spectra are normalized with the peak height of the 1466 cm^{-1} band.

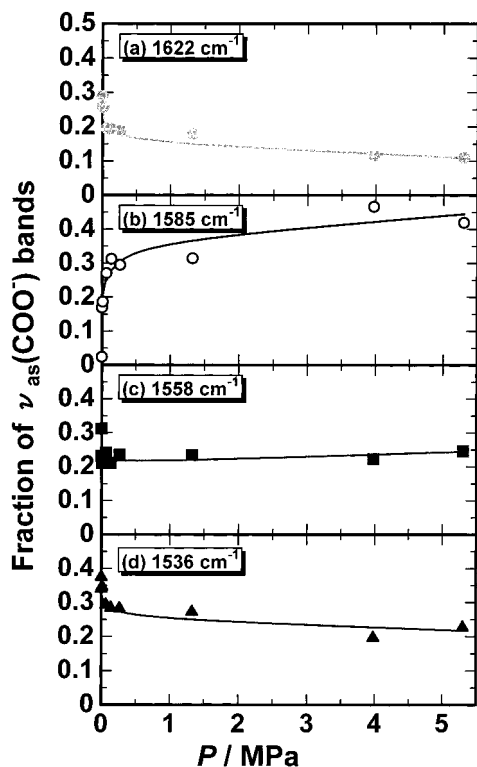


Figure 9. Plots of the fraction of $\nu_{\text{as}}(\text{COO}^-)$ bands at (a) 1622 (●), (b) 1585 (○), (c) 1558 (■), and (d) 1536 cm^{-1} (▲) as a function of pressure applied at 403 K. The fractions are calculated on the basis of integrated absorbance, and solid curves are only guides for the eye.

Coleman's type and the 1558 cm^{-1} component (and the 1536 cm^{-1} , overlapped with the 1536 cm^{-1} band of Coleman's type) to a simple hexacoordination form of $(-\text{COO}^-)_2\text{Zn}(\text{II})(-\text{COOH})$.¹¹ The ratio of the integrated absorbance of the 1536 cm^{-1} band to that of the 1622 cm^{-1} band roughly fell in the range of $2/(1 \pm 0.2)$, but with a slight increase with increasing pressure when looked at closer. Ishioka et al. reported that the relative integrated absorbances of the 1622, 1558, and 1536 cm^{-1} band components show a fixed ratio of 5.2:8:9 during water absorption process of the sample and thus concluded that those three components have the same origin.¹² However, none of such relations were obtained in the present work, where the pressure applied in the melt was varied.

Dependence of Equilibrium Constant on the Pressure in the Melt. In Figure 9b, it should be noted that the fraction of the 1585 cm^{-1} band component is 0.17 at $P = 0.0007$ MPa and reaches ~ 0.45 at $P = 5.4$

MPa, more than twice the value at $P = 0.0007$ MPa. Although the real system is not so simple, as already pointed out above, we assume here the presence of only two coordination states, tetra- and hexacoordination states, for simplicity, where the 1585 cm^{-1} band component is related to the tetracoordination state and three components at 1622, 1558, and 1536 cm^{-1} are involved in the hexacoordination state(s). Hence, the fraction of the 1585 cm^{-1} component and its change with P directly reflect a shift of the equilibrium between the two coordination states.

Our preliminary EXAFS studies revealed that the total coordination number in the first coordination shell around zinc(II) changes from 4.8 to 3.0, a $\sim 40\%$ decrease, when the pressure is increased from $P = 0.0007$ to 4 MPa.¹⁹ In the EXAFS studies, the radial structure function peak corresponding to the first coordination shell around zinc(II) was reproduced reasonably only by assuming two zinc(II)–oxygen bonds of 1.98–1.99 and 2.24–2.25 Å, but not by one type of zinc(II)–oxygen bond. On the other hand, the average coordination number estimated from the present IR studies is calculated as

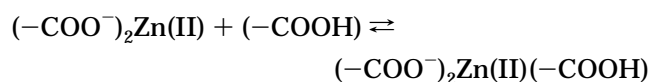
$$(4 \times 0.17/2 + 6 \times 0.83/3)/(0.17/2 + 0.83/3) = 5.5 \quad \text{for } P = 0.0007 \text{ MPa}$$

and

$$(4 \times 0.45/2 + 6 \times 0.55/3)/(0.45/2 + 0.55/3) = 4.9 \quad \text{for } P = 4 \text{ MPa}$$

The estimation shows a $\sim 10\%$ decrease of the coordination number with increasing pressure. Thus, there still remains a discrepancy on the quantitative basis, but the trends observed by the two studies are identical. Therefore, it is concluded that the transformation induced by pressure applied in the melt is accompanied by a change in the coordination number of the first coordination shell around zinc(II).

The equilibrium constant (K) for the following simplified equilibrium



was estimated and plotted vs the pressure applied in the melt in Figure 10. As clearly seen in (a), the value of K first rapidly decreases with increasing pressure P up to around $P = 0.25$ MPa, and after that, the decrease with P becomes very gradual. The $\log K$ vs $\log P$ plot, in (b), is approximately reproduced by a straight line,

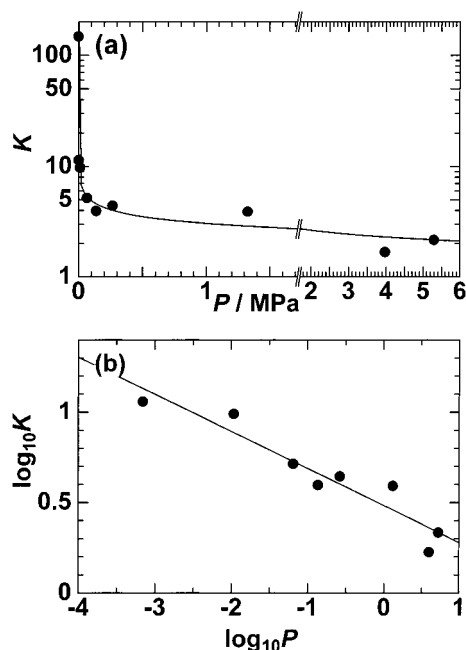


Figure 10. Dependence of the equilibrium constant K on pressure P : (a) $\log K$ vs P plot and (b) $\log K$ vs $\log P$ plot. The solid curve represents an equation of $\log K = 0.48 - 0.20 \log P$ (see text).

corresponding to an equation of $\log K = 0.48 - 0.20 \log P$, and thus, $K \propto P^{-0.20}$ was obtained. At this stage, however, the physical meaning of this relation is uncertain, and the next step is to clarify the molecular basis of this pressure-induced coordinational change.

Concluding Remarks

The present IR studies have elucidated an interesting phenomenon that the coordination structure around zinc(II) in the E-0.054MAA-0.6Zn ionomer is changed by pressure P applied in the melt, and when keeping the pressure on cooling, the coordination structure around zinc(II) almost retains the state determined in the melt to room temperature, and moreover, the state remains unchanged at room temperature when the pressure is released and/or reverted to the atmospheric pressure ($P = 0.1$ MPa). Although the assignment of the $\nu_{\text{as}}(\text{COO}^-)$ band components still has some problems, we assign the 1585 cm^{-1} band to a tetracoordination state, and three bands at 1624 , ~ 1560 , and 1538 cm^{-1} (which correspond to the resolved components at 1622 , 1558 , and 1536 cm^{-1} , respectively, in the curve-fitting results) are all involved in hexacoordination states such as a simple form of $(-\text{COO}^-)_2\text{Zn(II)}(-\text{COOH})$ and Coleman's type. Thus, it has been revealed that the pressure in the melt affects an equilibrium between the tetracoordinated and hexacoordinated zinc(II) cations, and increasing the pressure increases the presence of the former species. The curve-fitting results show that the fraction of the tetracoordination state is 0.17 for $P = 0.0007$ MPa and ~ 0.45 for $P = 5.4$ MPa, more than twice the value for $P = 0.0007$ MPa.

A remarkable feature of this pressure-induced coordinational change is that even exposure to atmospheric pressure is enough to change the coordination structure largely. However, the present phenomenon is not connected to some adduct formation of gas molecules such as O_2 that is often seen for oxygen-carrier transition-metal porphyrin complexes.²⁷ On the other hand, the

pressure-induced coordinational change of the zinc(II)-neutralized ionomer seems essentially different from the observation that, for example, zinc(II) oxide changes its coordination number from 4 to 6 at ~ 10 MPa and at ~ 600 K,²⁸ where the value of the pressure applied is much higher than that of our case. Very recently, we found that some zinc(II) complexes with an analogous local structure to this ionomer also show a similar pressure behavior, and the pressure-induced coordinational change is not limited to the ionomeric system. With this in mind, it is of much interest to elucidate the relationships between the coordination structure of some metal complexes and its activity to pressure, and such an investigation is currently in progress in our laboratories.

The coordinational change is strongly dependent on the temperature at which the pressure is applied, when the temperature is below the melting temperature T_m of polyethylene crystalline region which coexists in the sample. This result clearly indicates that the polyethylene crystalline region acts as a physical cross-link of the backbone, which in turn severely constrains the transformation of the coordination structure around zinc(II) with pressure at low temperatures. At this point, it can be said that some aspects of this interesting phenomenon is characteristic of zinc(II) carboxylates in zinc(II) salts of E-MAA ionomers, not seen for the corresponding low-molecular-mass analogues.

To clarify the mechanism or origin of this interesting phenomenon, further studies are apparently necessary. The next article will report how this phenomenon depends on the ionomer composition such as the degree of neutralization and MAA content.

Acknowledgment. The authors are indebted to Prof. Yoshihiro Sugi and Yoshihiro Kubota (Gifu University) for permitting us the use of an autoclave, to Ms. Eriko Sawada, Mr. Kazuhiro Miyata, Katsuomi Shimabayashi, and Daisuke Matsuoka (Gifu University) for their experimental aids, and to Prof. J. Umemura (Institute for Chemical Research, Kyoto University) for his valuable discussions and encouragement. The authors are also indebted to Mr. Hideki Hashimoto (Toray Research Center) for measuring EXAFS spectra.

References and Notes

- (1) For example: (a) Rees, R. W.; Vaughan, D. J. *Polym. Prepr. (Am. Chem. Soc., Div. Polym. Chem.)* **1965**, *6*, 287. (b) Eisenberg, A. *Macromolecules* **1970**, *3*, 147. (c) *Ionomers: Characterization, Theory, and Applications*; Schlick, S., Ed.; CRC Press: Boca Raton, FL, 1996.
- (2) For example: Yarusso, D. J.; Cooper, S. L. *Macromolecules* **1983**, *16*, 1871.
- (3) Kutsumizu, S.; Tagawa, H.; Muroga, Y.; Yano, S. *Macromolecules* **2000**, *33*, 3818.
- (4) For example: Brozoski, B. A.; Coleman, M. M.; Painter, P. C. *Macromolecules* **1984**, *17*, 230.
- (5) For example: (a) Pineri, M.; Meyer, C.; Levelut, A.-M.; Lambert, M. *J. Polym. Sci., Polym. Phys. Ed.* **1974**, *12*, 115. (b) Szajdzinska-Pietek, E.; Schlick, S. In ref 1c, pp 135–163.
- (6) For example: Yarusso, D. J.; Ding, Y. S.; Pan, H. K.; Cooper, S. L. *J. Polym. Sci., Polym. Phys. Ed.* **1984**, *22*, 2073.
- (7) Yano, S.; Hirasawa, E.; Tadano, K.; Yamauchi, J.; Kamiya, Y. *Macromolecules* **1989**, *22*, 3186.
- (8) Kutsumizu, S.; Watanabe, Y.; Yano, S.; Tachino, H.; Hara, H.; Kutsuwa, Y. *J. Mater. Sci.* **1997**, *32*, 99.
- (9) Yano, S.; Tadano, K.; Hirasawa, E.; Yamauchi, J. *Macromolecules* **1990**, *23*, 4872.
- (10) Kutsumizu, S.; Kimura, H.; Mohri, F.; Hara, H.; Tachino, H.; Hirasawa, E.; Yano, S. *Macromolecules* **1996**, *29*, 4324.
- (11) Coleman, M. M.; Lee, J. Y.; Painter, P. C. *Macromolecules* **1990**, *23*, 2339.

- (12) Ishioka, T. *Polym. J.* **1993**, *25*, 1147.
- (13) Yano, S.; Nakamura, M.; Kutsumizu, S. *Chem. Commun.* **1999**, 1465.
- (14) Kutsumizu, S.; Tadano, K.; Matsuda, Y.; Goto, M.; Tachino, H.; Hara, H.; Hirasawa, E.; Tagawa, H.; Muroga, Y.; Yano, S. *Macromolecules* **2000**, *33*, 9044.
- (15) Tsunashima, K.; Nishioji, H.; Hirasawa, E.; Yano, S. *Polymer* **1992**, *33*, 1809.
- (16) Grady, B. P.; Floyd, J. A.; Genetti, W. B.; Vanhoorne, P.; Register, R. A. *Polymer* **1999**, *40*, 283.
- (17) Grady, B. P. *Macromolecules* **1999**, *32*, 2983.
- (18) Welty, A.; Ooi, S.; Grady, B. P. *Macromolecules* **1999**, *32*, 2989.
- (19) Hashimoto, H.; Kutsumizu, S.; Tsunashima, K.; Yano, S. *Macromolecules*, in press.
- (20) Hirasawa, E.; Yamamoto, Y.; Tadano, K.; Yano, S. *J. Appl. Polym. Sci.* **1991**, *42*, 351.
- (21) Lee, J. Y.; Painter, P. C.; Coleman, M. M. *Macromolecules* **1988**, *21*, 346.
- (22) Minami, S. *Processing of Wave Signals for Scientific Measurements*; CQ Press: Tokyo, 1986 [in Japanese].
- (23) (a) Davidon, W. C. *AEC Research and Development Report* **1959**, ANL-5990. (b) Fletcher, R.; Powell, M. J. D. *Comput. J.* **1963**, *6*, 163.
- (24) Ng, J. B.; Shurvell, H. F. *J. Phys. Chem.* **1987**, *91*, 496.
- (25) Tanaka, N.; Kitano, H.; Ise, N. *J. Phys. Chem.* **1990**, *94*, 6290.
- (26) (a) Tadano, K.; Hirasawa, E.; Yamamoto, Y.; Yamamoto, H.; Yano, S. *Jpn. J. Appl. Phys.* **1987**, *26*, L1440. (b) Tadano, K.; Hirasawa, E.; Yamamoto, H.; Yano, S. *Macromolecules* **1989**, *22*, 226.
- (27) Voet, D.; Voet, J. G. *Biochemistry*; Wiley: New York, 1990.
- (28) Bates, C. H.; White, W. B.; Roy, R. *Science* **1962**, *137*, 993.

MA001342S